

## **Electronic supplementary information**

### **Ferrocene based metal-organic framework nanosheets loading**

### **palladium as super-high active hydrogenation catalyst**

Zheng Deng,<sup>[a]</sup> Haojie Yu\*,<sup>[a]</sup> Li Wang\*,<sup>[a]</sup> Jiyang Liu,<sup>[a]</sup> and Kenneth J Shea<sup>[b]</sup>

<sup>a</sup>: State Key Laboratory of Chemical Engineering, College of Chemical and Biological Engineering, Zhejiang University, Hangzhou 310027, China

<sup>b</sup>: Department of Chemistry, University of California, Irvine, Irvine, California 92697, United States

## **S1. Materials and Methods**

Zirconium tetrachloride ( $\text{ZrCl}_4$ ) and potassium tetrachloropalladate ( $\text{K}_2\text{PdCl}_4$ ) were obtained from Aladdin. Acetic acid ( $\text{CH}_3\text{COOH}$ ), dimethyl formamide (DMF) and styrene were purchased from Sinopharm Chemical Reagent Co., Ltd. 1,1'-ferrocenedicarboxylic acid ( $\text{Fc}(\text{COOH})_2$ ) was purchased from Energy Chemical. All the chemicals were used without further purification.

The powder X-ray diffraction data were collected on X-pert Powder diffractometers using  $\text{Cu K}\alpha$  radiation sources ( $\lambda = 1.54178 \text{ \AA}$ ). Thermal gravimetric analysis (TGA) was performed on TA-Q500 (Mettler-Toledo) at a heating rate of  $10 \text{ }^\circ\text{C}/\text{min}$  in nitrogen atmosphere. Scanning electron microscopy (SEM) images were taken on Utral 55 ( $V=5 \text{ kV}$ ). Transmission electron microscope images were taken using HT7700 TEM. High-resolution transmission electron microscope (HR-TEM) images were obtained from JEM 2100F using ultrathin carbon supporting film as a support. Atomic force microscopy (AFM) images were taken SPI-3800N using tapping mode.  $\text{N}_2$  sorption isotherms were recorded on a TriStar II instrument. X-ray photoelectron spectroscopy (XPS) spectra were acquired with a VG ESCALAB MARK II XPS system. Gas chromatography test were conducted on Agilent GC 6890 using ethanol as solvent and dodecane as internal standard. Inductively coupled plasma atomic emission spectra (ICP-AES) were required on iCAP6300 after samples were digested in aqua regia at  $80 \text{ }^\circ\text{C}$  for 12 h.

## **S2. Experimental Section**

### **S2.1 Synthesis of Zr-Fc MOF**

Typically,  $\text{ZrCl}_4$  (116.5 mg, 0.5 mmol),  $\text{Fc}(\text{COOH})_2$  (137 mg, 0.5 mmol) and different amount of acetic acid (varied from 0-150 mmol) were dissolved in DMF (15 mL) in a 25 mL Teflon container. Then, it was capped and put inside a hydrothermal reactor, which was subsequently

heated at 120 °C for different time. The resulting crystals were collected and centrifuged (3000 rpm, 30 min). Then, the precipitate was dispersed in DMF (30 mL) again. This centrifuge-disperse process was repeated for 3 times. The final Zr-Fc MOF (wet sample) was obtained after removal of the supernatant. Notably, for SEM, TEM, HR-TEM and AFM analysis, the wet sample was dispersed in ethanol via ultra-sonication method. Typically, about 1 mg wet sample was transferred into a 3 mL vial, into which about 2 mL ethanol was added. The resultant mixture was sonicated at room temperature for 20 min. The obtained dispersion was properly diluted before preparing samples for test. For XRD analysis, the wet sample was further dried under vacuum at 35 °C for 24h.

## **S2.2 Preparation of Pd/Zr-Fc MOF nanosheets composites**

Pd/Zr-Fc MOF nanosheets composites were prepared through *in situ* reduction of Pd<sup>2+</sup> (K<sub>2</sub>PdCl<sub>4</sub>) into Pd by Zr-Fc MOF. Typically, about 200 mg Zr-Fc MOF (thickness: about 11.6 nm) was dispersed in 800 mL deionized water by ultra-sonication method for 30 min. The obtained dispersion was divided into four equal parts, into which different volumes (2.5 mL, 5.0 mL, 15 mL and 30 mL) of K<sub>2</sub>PdCl<sub>4</sub> aqueous solution (2mg/mL) were added by drop-wise respectively. After being stirred at 30 °C for 3h, those dispersion were filtered through PC membranes (pore width: 220 nm), and the filter residues were washed with 100 mL deionized water for three times respectively. The obtained wet residues were collected and dispersed again in ethanol for further TEM and catalysis study. To study the effects of Zr-Fc MOF thickness on catalytic behavior of Pd/Zr-Fc MOF composites, Zr-Fc MOFs with different thickness (about 4.4 nm and 15.9 nm) were used for loading Pd in a similar procedure. Pd@UiO-66 was prepared in a two-step procedure. Firstly, UiO-66 was dispersed in deionized water by ultra-sonication followed by addition of K<sub>2</sub>PdCl<sub>4</sub> aqueous solution.

Pd<sup>2+</sup>@UiO-66 was obtained after centrifugation (10000 rpm, 10 min), which was further reduced into Pd@UiO-66 by NaBH<sub>4</sub>.

### **S2.3 Hydrogenation reaction of styrene catalyzed by Pd/Zr-Fc MOF nanosheets composites**

The hydrogenation of styrene was conducted according to a reported literature <sup>[1]</sup> with little modification. Typically, a 50 mL three neck flask equipped with a rubber bladder was immersed in 30 °C oil bath and purged with H<sub>2</sub> for several times. Then, a certain amount of Pd/Zr-Fc MOF nanosheets were dispersed in 10-20 mL ethanol via ultra-sonication (r.t., 30 min). Subsequently, 1.0 mL of the Pd/Zr-Fc MOF dispersion was injected into the flask followed by addition of 19 mL of ethanol. Meanwhile, another 1.0 mL of the Pd/Zr-Fc MOF dispersion was transferred into a 10 mL vial, which was placed onto a 60 °C oven for 24 h to evaporate ethanol. Then, the residue was digested at 80 °C for 12 h using aqua regia (mixture of 6 mL 36.6 wt. % HCl and 2 mL 65 wt. % HNO<sub>3</sub>) for ICP-AES analysis. The reaction was started when styrene (70 µL, 0.6 mmol) was added into the flask. After a certain time, 0.8-0.9 mL of the mixture was taken for GC analysis after Pd/Zr-Fc MOF nanosheets were filtered off via filtration through a 0.22 µm filter. The hydrogenation reaction of styrene was also catalyzed by Pd@UiO-66 and Zr-Fc MOF respectively in a similar procedure.

### **S3. Crystal data and structure refinement details.**

A possible crystal structure of Zr-Fc MOF was promoted through Materials Studio (MS) 8.0 based on powder XRD refinement according to the reference <sup>[2]</sup>. The procedure to obtain the crystal structure of Zr-Fc MOF was as follow.

(a) Indexing the unite cell. The XRD pattern of Zr-Fc MOF was imported into MS and was used for Reflex Powder Indexing after its background was subtracted. As shown at Table S1, the

indexed peaks were quite close to the experimental data. Subsequently, we obtained the unit cell parameters ( $a=b=c=14.116 \text{ \AA}$ ,  $\alpha=\beta=\gamma=90^\circ$ ) of Zr-Fc MOF. It is worth to mention that the obtained value for a, b and c were  $14.116 \text{ \AA}$ , which was close to the lattice spacing ( $14.6 \text{ \AA}$ ) of Zr-Fc MOF nanosheets observed in HR-TEM images (Fig. 2c).

(b) Building a rough crystal structure. We found that the XRD pattern of Zr-Fc MOF and the UMCM-309a from the literature [2] share some similarities. Thus, UMCM-309a was employed as a parent crystal model to build the rough crystal structure of Zr-Fc MOF. To be specifically, the crystal structure of UMCM-309a was built in MS, then its linkers (BTB) was replaced with  $\text{Fc}(\text{COOH})_2$  or acetic acid while  $\text{Zr}_6$  cluster remained unchanged.

**Table S1** Peaks used for Reflex Powder Indexing.

h	k	l	2-theta exp.	2-theta calc.	Difference
1	0	0	6.2390	6.2560	-0.017
1	1	0	8.8870	8.8520	0.035
2	0	0	12.497	12.531	-0.034
2	1	0	14.006	14.017	-0.011
2	2	0	17.828	17.757	0.071
3	1	0	19.903	19.873	0.030
3	2	0	22.739	22.694	0.045
4	2	0	28.227	28.249	-0.022
5	2	0	34.162	34.178	-0.016

(c) Optimization of the rough crystal structure. Forcite Calculation of MS was applied for both energy and geometry optimization using a Universal forcefield with convergence quality changed from coarse to ultra-fine. Notably, the unit cell parameters were set to be  $a=b=c=14.116 \text{ \AA}$ ,  $\alpha=\beta=\gamma=90^\circ$  and were not optimized.

(d) Refinement of the crystal structure. Powder Refinement of MS was used to refine the crystal structure of Zr-Fc MOF. A Rietveld refinement was applied to the model against the experimental XRD pattern of Zr-Fc MOF in the range of 5-40 degree. Atom position, atom occupancy and FWHM

were refined and the convergence quality was ultra-fine. After several trials, the calculated XRD pattern was in accord with the experimental one with  $R_{wp}=13.06\%$ ,  $R_{wp}$  (w/o bck) =13.49% and  $R_p=29.98\%$ . The detailed unite cell parameters and atomic coordinates of Zr-Fc MOF were listed at Table S2.

**Table S2** Refined unite cell parameters and atomic coordinates of Zr-Fc MOF.

Formula sum	Zr <sub>3</sub> FeC <sub>14</sub> O <sub>16</sub> H <sub>8</sub>							
Formula weight	761.6 g/mol							
Crystal system	triclinic							
Space-group	P 1 (1)							
Cell parameters	a=14.1161 Å b=14.1161 Å c=14.1161 Å α=90.00° β=90.00° γ=90.00°							
Cell ratio	a/b=1.0000 b/c=1.0000 c/a=1.0000							
Cell volume	2812.83 Å <sup>3</sup>							
Atomic parameters								
Atom	Ox.	Wyck.	Site	S.O.F.	x/a	y/b	z/c	U [Å <sup>2</sup> ]
O1		1a	1	0	1.02814	0.76613	0.08332	0.0000
O2		1a	1	0	1.09785	0.75286	-0.06034	0.0000
Zr3		1a	1	0	0.96326	0.89871	0.06713	0.0000
C4		1a	1	0	1.07070	0.71774	0.01913	0.0000
O5		1a	1	0.11	0.96329	0.85311	-0.07247	0.0000
O6		1a	1	0.02	0.92175	0.81095	0.18055	0.0000
O7		1a	1	0.01	0.98368	0.96186	0.20064	0.0000
O8		1a	1	0.09	0.22833	0.17395	-0.00808	0.0000
O9		1a	1	0	0.16969	0.20456	-0.15504	0.0000
Zr10		1a	1	0.01	0.13742	0.06374	0.03414	0.0000
C11		1a	1	0	0.22840	0.21946	-0.08725	0.0000
O12		1a	1	0.01	0.15551	0.03501	-0.10928	0.0000
O13		1a	1	0.07	0.12409	0.15985	0.14765	0.0000
O14		1a	1	0.05	0.21292	1.03688	0.16024	0.0000
O15		1a	1	0.07	0.75957	0.13384	-0.00926	0.0000
O16		1a	1	0.02	0.73367	0.01347	-0.11371	0.0000
Zr17		1a	1	0.01	0.90585	0.12677	0.01357	0.0000
C18		1a	1	0	0.70625	0.08535	-0.06491	0.0000
O19		1a	1	0	0.90028	0.10507	-0.13166	0.0000
O20		1a	1	0.02	0.92563	0.13480	0.16108	0.0000
O21		1a	1	0.05	-0.18504	0.22697	0.07675	0.0000
O22		1a	1	0	-0.01932	0.25718	-0.16849	0.0000
O23		1a	1	0	-0.09032	0.27010	-0.02540	0.0000
Zr24		1a	1	0	0.04506	0.12434	-0.15254	0.0000
C25		1a	1	0	-0.06251	0.30534	-0.10462	0.0000

O26	1a	1	0.04	0.04499	0.16993	-0.01296	0.0000
O27	1a	1	0.04	0.08635	0.21208	-0.26606	0.0000
O28	1a	1	0.01	0.02458	0.06152	-0.28616	0.0000
O29	1a	1	0.17	0.78002	0.84900	-0.07726	0.0000
O30	1a	1	0	0.83888	0.81814	0.06955	0.0000
Zr31	1a	1	0	0.87085	0.95927	-0.11953	0.0000
C32	1a	1	0	0.78007	0.80339	0.00186	0.0000
O33	1a	1	0.06	0.85278	0.98802	0.02387	0.0000
O34	1a	1	0.03	0.88447	0.86311	-0.23298	0.0000
O35	1a	1	0.05	0.79519	-0.01398	-0.24559	0.0000
O36	1a	1	0.15	0.24862	0.88893	-0.07603	0.0000
O37	1a	1	0.03	0.27457	1.00944	0.02831	0.0000
Zr38	1a	1	0.01	0.10240	0.89626	-0.09904	0.0000
C39	1a	1	0	0.30196	0.93746	-0.02038	0.0000
O40	1a	1	0	0.10800	0.91796	0.04619	0.0000
O41	1a	1	0	0.08269	0.88856	-0.24659	0.0000
O42	1a	1	0.02	1.19342	0.79613	-0.16211	0.0000
O43	1a	1	0.05	0.00014	0.04249	0.09829	0.0000
O44	1a	1	0.04	0.00811	-0.01942	-0.18367	0.0000
Fe45	1a	1	0	-0.99600	0.51155	1.95722	0.0000
C46	1a	1	0	-0.91483	0.61620	2.03566	0.0000
C47	1a	1	0	-0.85182	0.55855	1.98780	0.0000
C48	1a	1	0	-0.86151	0.46805	2.02343	0.0000
C49	1a	1	0	-0.93001	0.46984	2.09301	0.0000
C50	1a	1	0	-0.96267	0.56150	2.10115	0.0000
H51	1a	1	0	-0.80440	0.57989	1.93149	0.0000
H52	1a	1		-0.95458	0.40958	2.13352	0.0000
H53	1a	1	0.43	-1.01746	0.58553	2.14910	0.0000
C54	1a	1	0	-1.06204	0.55320	1.82148	0.0000
C55	1a	1	0	-1.13047	0.55498	1.89117	0.0000
C56	1a	1	0	-1.14015	0.46448	1.92676	0.0000
C57	1a	1	0	-1.07713	0.40688	1.87888	0.0000
C58	1a	1	0	-1.02938	0.46154	1.81331	0.0000
H59	1a	1	0.97	-1.03745	0.61346	1.78101	0.0000
H60	1a	1	0	-1.18750	0.44308	1.98316	0.0000
H61	1a	1	0.76	-0.97465	0.43747	1.76532	0.0000
H62	1a	1	0	-0.82324	0.40616	2.00006	0.0000
H63	1a	1	0	-1.16875	0.61685	1.91457	0.0000
Fe64	1a	1	0	1.50412	1.01135	0.95745	0.0000
C65	1a	1	0.13	1.55480	1.14917	1.00267	0.0000
C66	1a	1	0.01	1.46383	1.16015	0.97052	0.0000
C67	1a	1	0	1.46104	1.13409	0.87605	0.0000
C68	1a	1	0	1.55080	1.10607	0.84998	0.0000
C69	1a	1	0	1.60765	1.11333	0.92924	0.0000

H70	1a	1	0	1.57137	1.07859	0.78142	0.0000
C71	1a	1	0	1.45727	0.91670	1.06490	0.0000
C72	1a	1	0	1.54703	0.88852	1.03898	0.0000
C73	1a	1	0.07	1.54437	0.86250	0.94449	0.0000
C74	1a	1	0.19	1.45346	0.87361	0.91220	0.0000
C75	1a	1	0	1.40052	0.90940	0.98556	0.0000
H76	1a	1	0	1.43662	0.94424	1.13341	0.0000
H77	1a	1	0	1.39885	1.13215	0.83139	0.0000
H78	1a	1	0	1.60914	0.89038	1.08376	0.0000
H79	1a	1	0	1.57885	1.16127	1.07446	0.0000
H80	1a	1	0.57	1.40484	1.18228	1.01364	0.0000
H81	1a	1	0.94	1.60338	0.84023	0.90146	0.0000
H82	1a	1	0	1.42951	0.86160	0.84036	0.0000
C83	1a	1	0	1.30026	1.29507	0.89805	0.0000
C84	1a	1	0	0.70834	0.72765	1.01648	0.0000

---



#### S4. Figures and tables

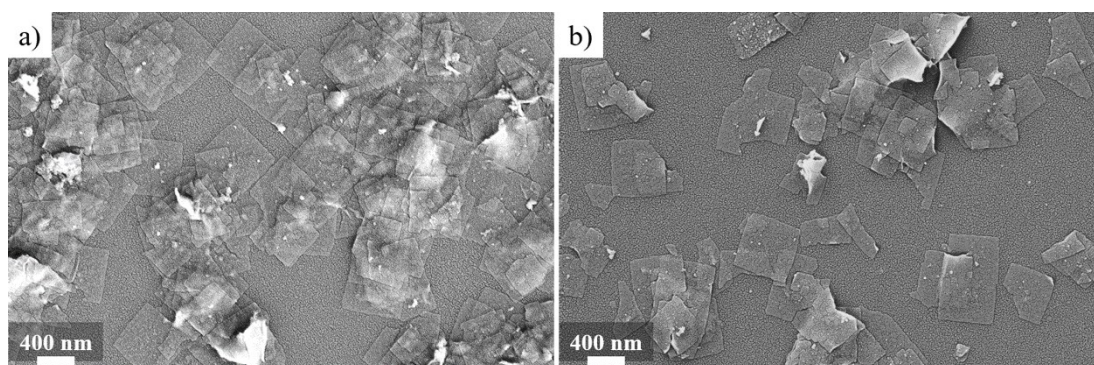


**Fig. S1** SEM images of Zr-Fc MOF ( $\text{CH}_3\text{COOH}/\text{ZrCl}_4=50$ ) before (a) and after (b) ultra-sonication.

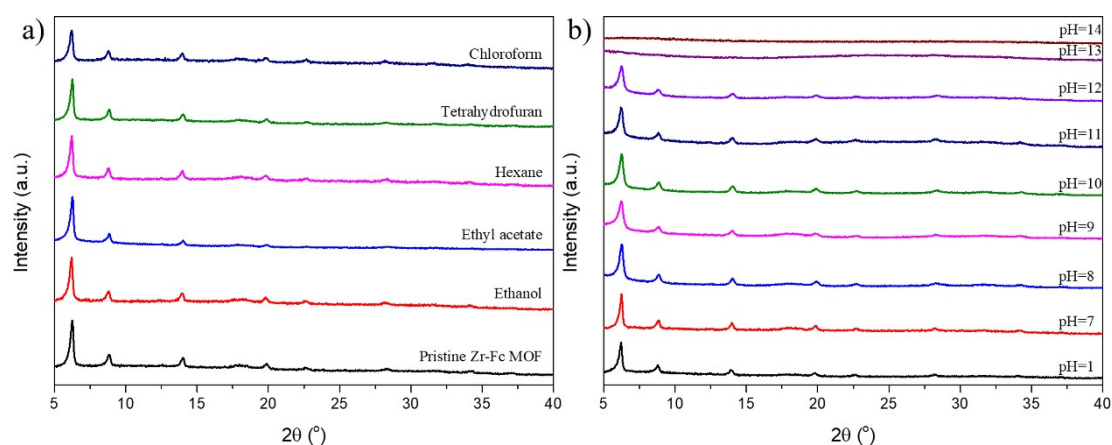


**Fig. S2** XRD patterns of Zr-Fc MOF nanosheets before and after being immersed into different organic solvents (a) or aqueous solutions with different pH value (b) for 24 h.

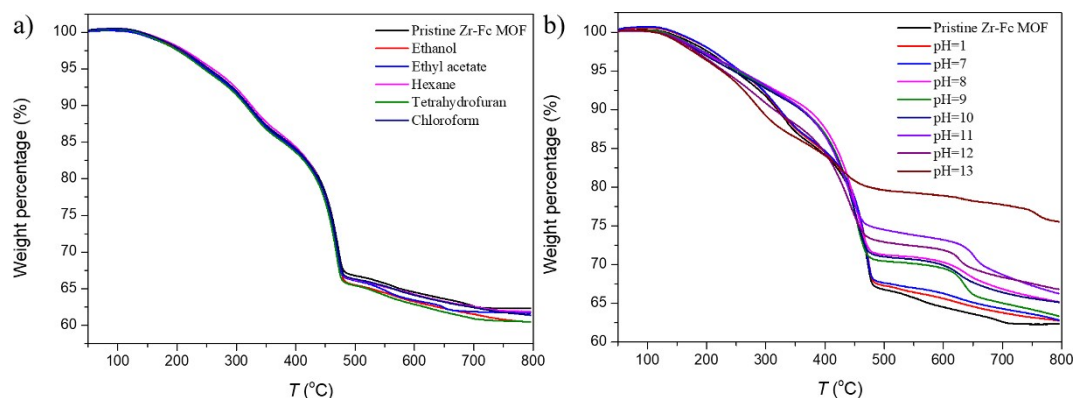


**Fig. S3** TGA curves of Zr-Fc MOF nanosheets before and after being immersed into different organic solvents (a) or aqueous solutions with different pH value (b) for 24 h. The percentage of ligand decreased when Zr-Fc MOF was immersed in aqueous solution with higher pH value. We speculated that some coordinating bonds between FcDA ligands and  $\text{Zr}_6$  clusters might be broken resulting in the loss of FcDA ligands at alkaline solution.

**Table S3** Experimental conditions for the synthesis of Zr-Fc MOF nanosheets under different molar ratio of  $\text{CH}_3\text{COOH}/\text{ZrCl}_4$ .

Runs	$\text{ZrCl}_4$		$\text{Fc}(\text{COOH})_2$		$\text{CH}_3\text{COOH}$		$\text{CH}_3\text{COOH}/\text{ZrCl}_4$	DMF	T	t
	mg	mmol	mg	mmol	mL	mmol	mol/mol	mL	°C	h
1	118.5	0.5	137.3	0.5	0	0	0	15	120	12
2	117.2	0.5	137.7	0.5	0.28	5.0	10	15	120	12
3	117.5	0.5	137.2	0.5	0.71	12.5	25	15	120	12
4	117.1	0.5	136.7	0.5	1.43	25	50	15	120	12
5	118.1	0.5	136.6	0.5	2.14	37.5	75	15	120	12
6	116.7	0.5	137.7	0.5	2.86	50	100	15	120	12
7	117.5	0.5	137.4	0.5	5.72	100	200	15	120	12
8	117.8	0.5	137.8	0.5	8.57	150	300	15	120	12

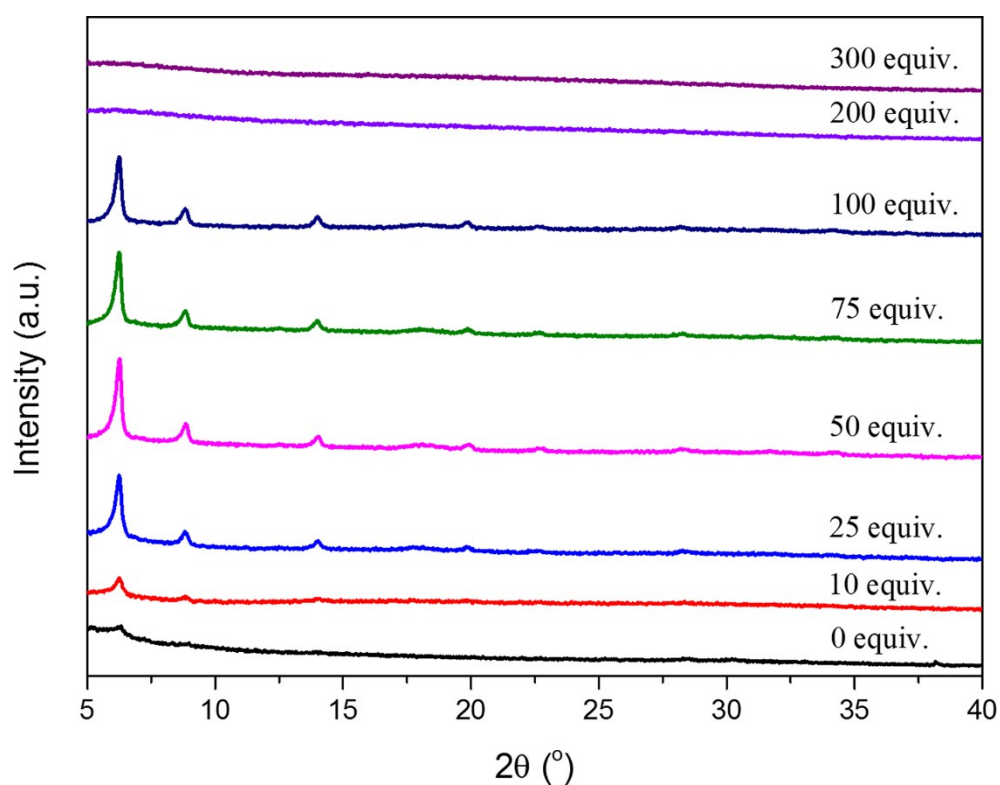


**Fig. S4** XRD patterns of Zr-Fc MOF nanosheets synthesized under different molar ratio of  $\text{CH}_3\text{COOH}/\text{ZrCl}_4$  (Run 1-8 at Table S3).

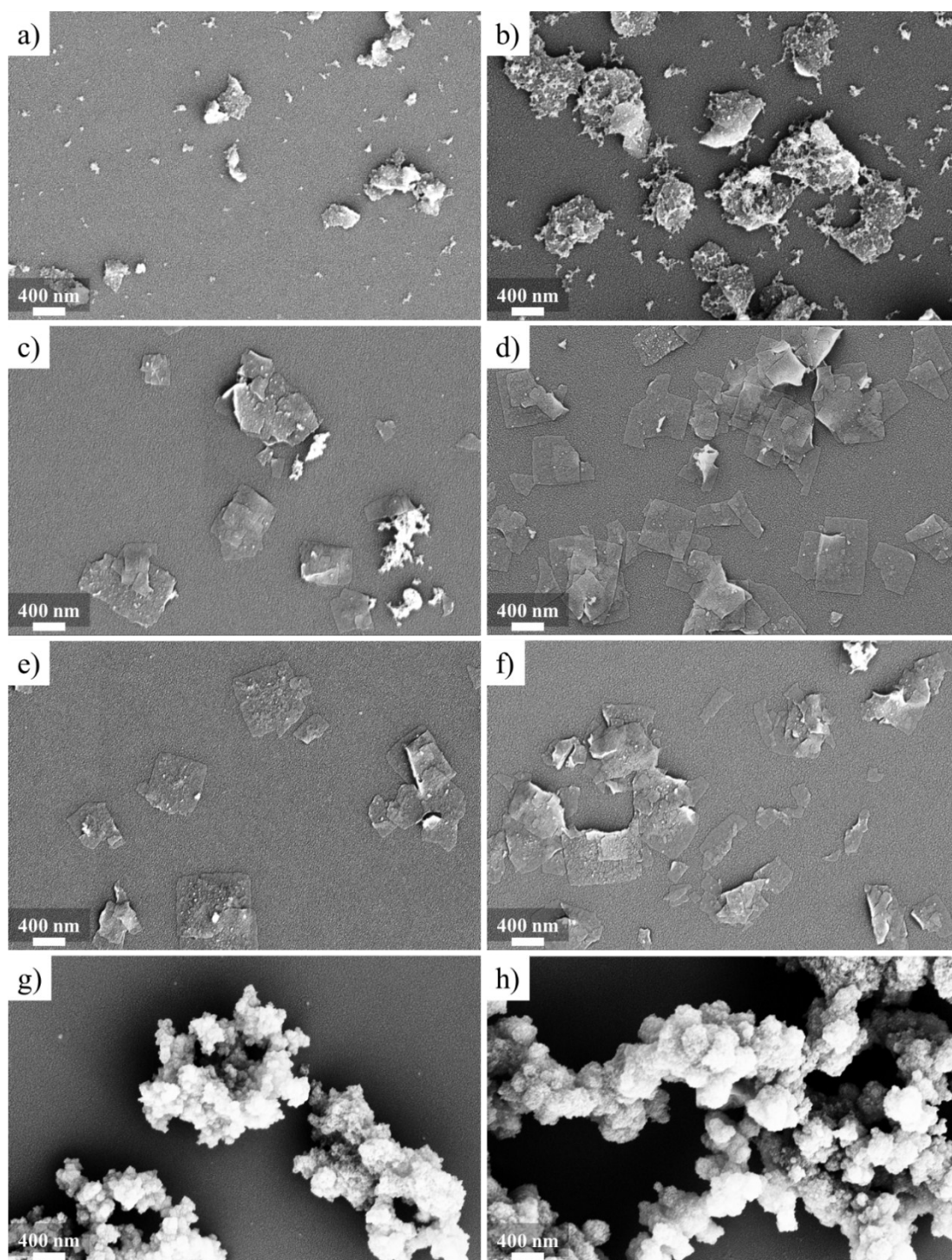


**Fig. S5** SEM images of Zr-Fc MOF nanosheets synthesized under different molar ratio of  $\text{CH}_3\text{COOH}/\text{ZrCl}_4$ . a) 0, b) 10, c) 25, d) 50, e) 75, f) 100, g) 200 and h) 300 (Run 1-8 at Table S3).

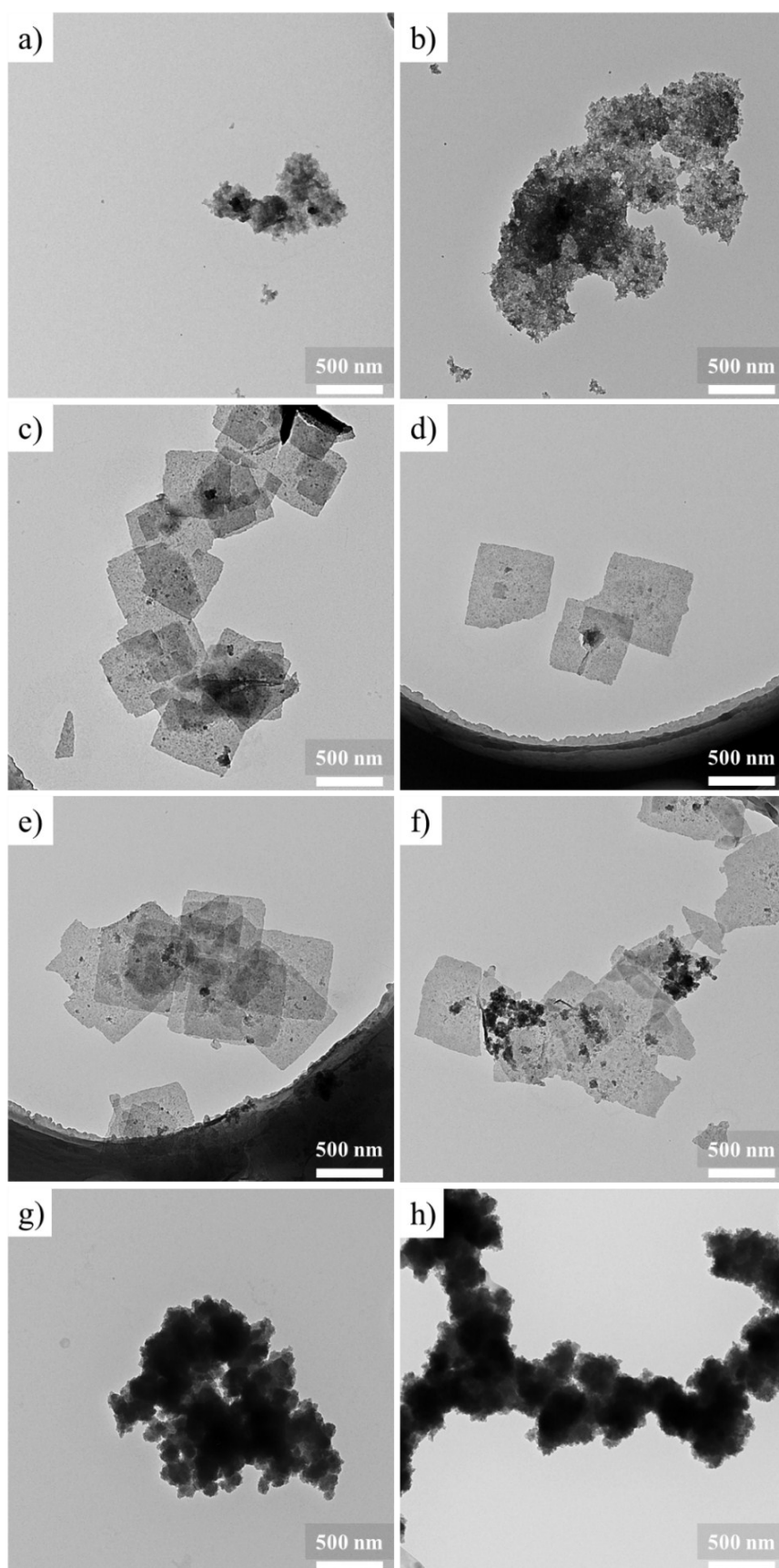


**Fig. S6** TEM images of Zr-Fc MOF nanosheets synthesized under different molar ratio of  $\text{CH}_3\text{COOH}/\text{ZrCl}_4$ . a) 0, b) 10, c) 25, d) 50, e) 75, f) 100, g) 200 and h) 300 (Run 1-8 at Table S3).



**Table S4** Experimental conditions for the synthesis of Zr-Fc MOF nanosheets under different reaction time (2-48h) and temperature (100-150 °C).

Runs	ZrCl <sub>4</sub>		Fc(COOH) <sub>2</sub>		CH <sub>3</sub> COOH		DMF	T	t
	mg	mmol	mg	mmol	mL	mmol	mL	°C	h
1	116.8	0.5	136.7	0.5	1.43	25	15	<b>100</b>	12
2	116.9	0.5	137.1	0.5	1.43	25	15	<b>110</b>	12
3	118.4	0.5	138.0	0.5	1.43	25	15	<b>130</b>	12
4	116.0	0.5	138.0	0.5	1.43	25	15	<b>140</b>	12
5	117.7	0.5	136.6	0.5	1.43	25	15	<b>150</b>	12
6	119.2	0.5	138.0	0.5	1.43	25	15	120	<b>2</b>
7	116.7	0.5	138.6	0.5	1.43	25	15	120	<b>3</b>
8	117.5	0.5	137.3	0.5	1.43	25	15	120	<b>6</b>
9	117.9	0.5	137.7	0.5	1.43	25	15	120	<b>12</b>
10	116.3	0.5	137.2	0.5	1.43	25	15	120	<b>24</b>
11	117.5	0.5	137.0	0.5	1.43	25	15	120	<b>48</b>

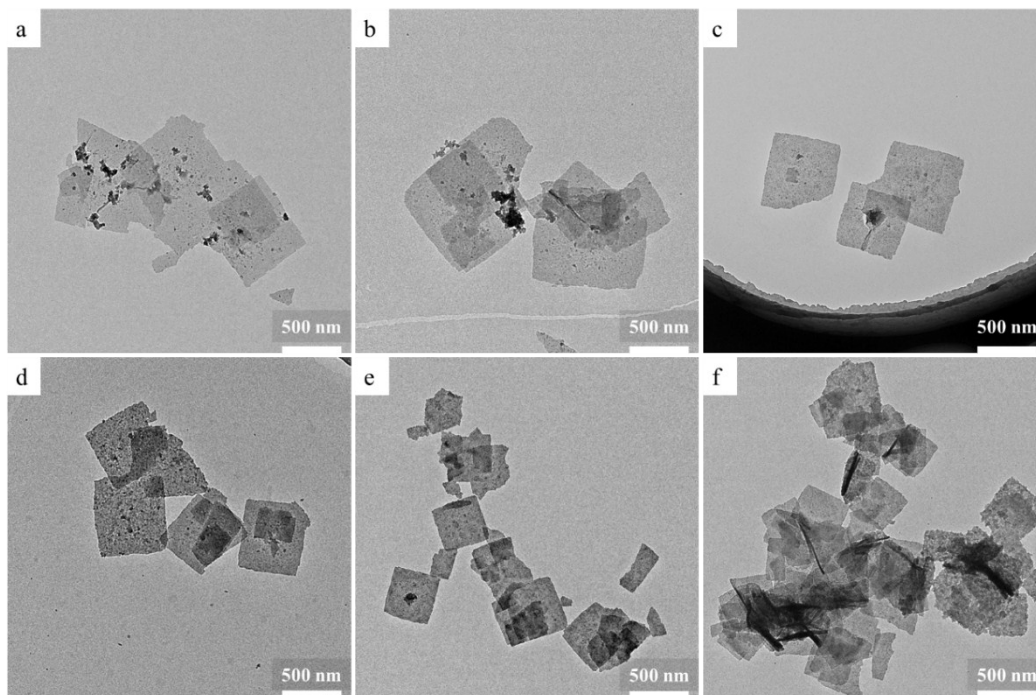


**Fig. S7** TEM images of Zr-Fc MOF nanosheets synthesized under different reaction temperature.

a) 100 °C, b) 110 °C, c) 120 °C, d) 130 °C, e) 140 °C and f) 150 °C (Run 1-5, 9 at Table S4).

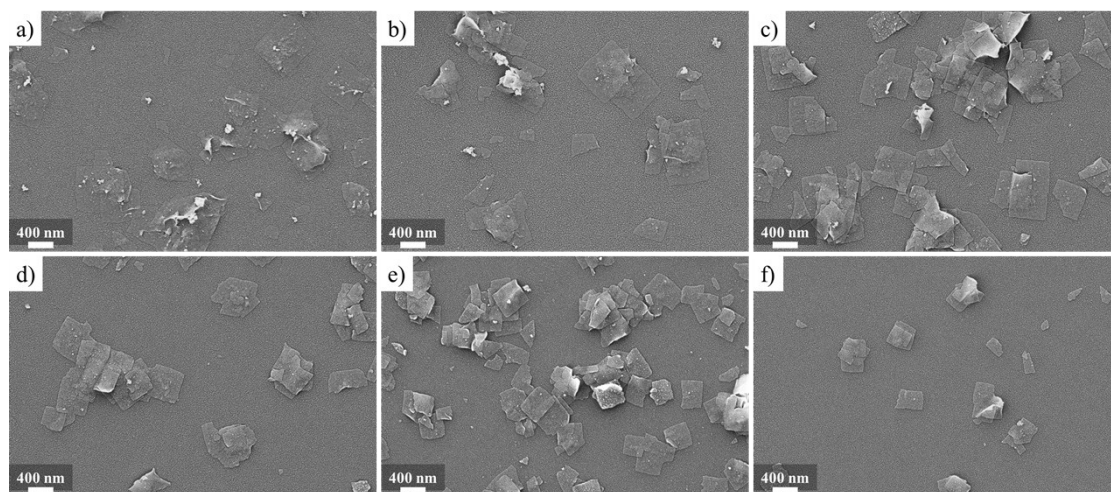


**Fig. S8** SEM images of Zr-Fc MOF nanosheets synthesized under different reaction temperature. a) 100 °C, b) 110 °C, c) 120 °C, d) 130 °C, e) 140 °C and f) 150 °C (Run 1-5, 9 at Table S4).

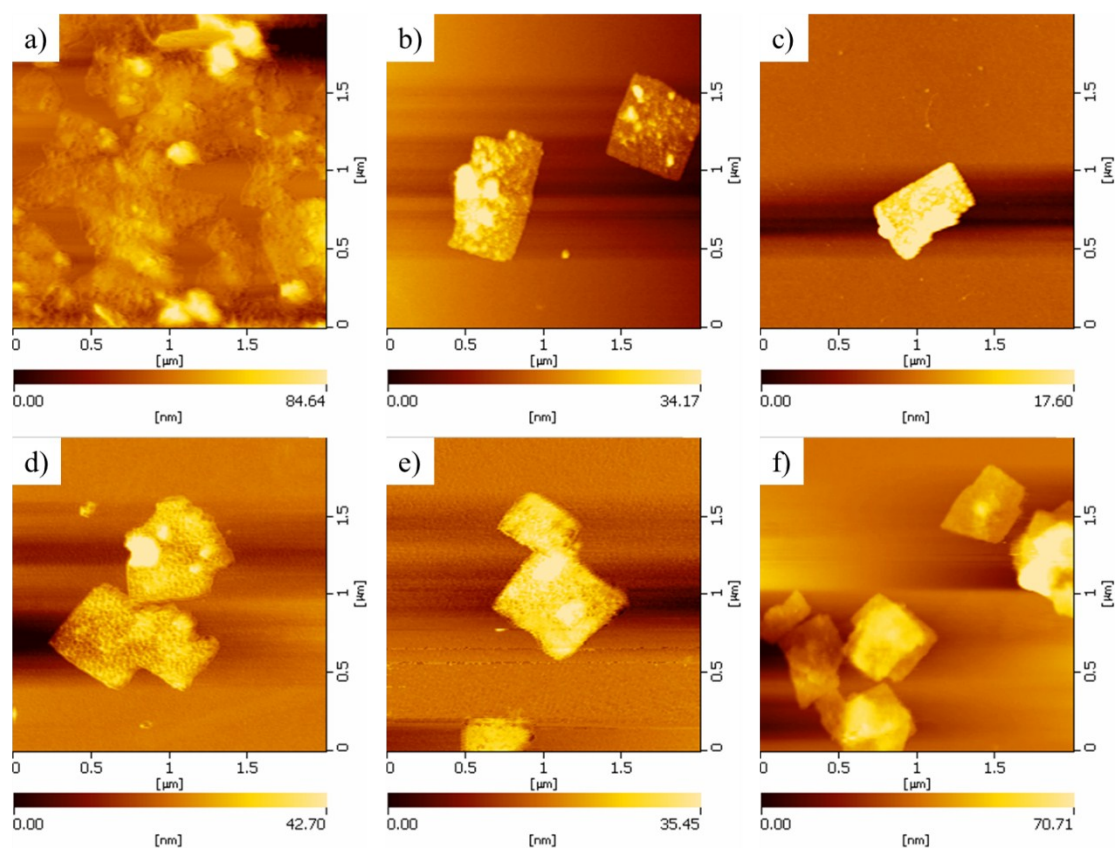


**Fig. S9** AFM height images of Zr-Fc MOF nanosheets synthesized under different reaction temperature. a) 100 °C, b) 110 °C, c) 120 °C, d) 130 °C, e) 140 °C and f) 150 °C (Run 1-5, 9 at Table S4).

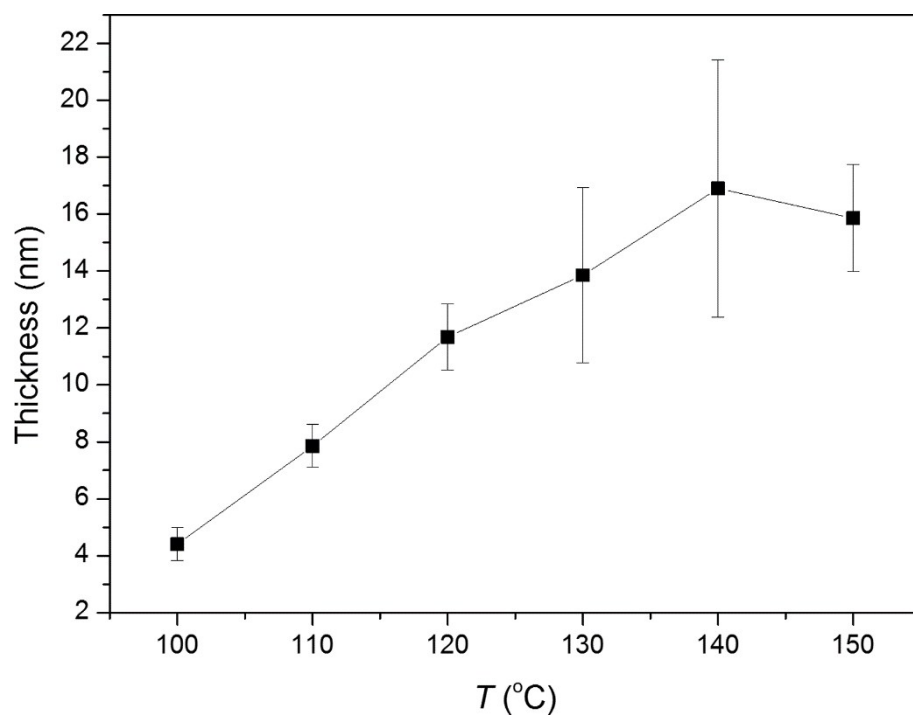


**Fig. S10** Thickness of Zr-Fc MOF nanosheets synthesized under different reaction temperature.

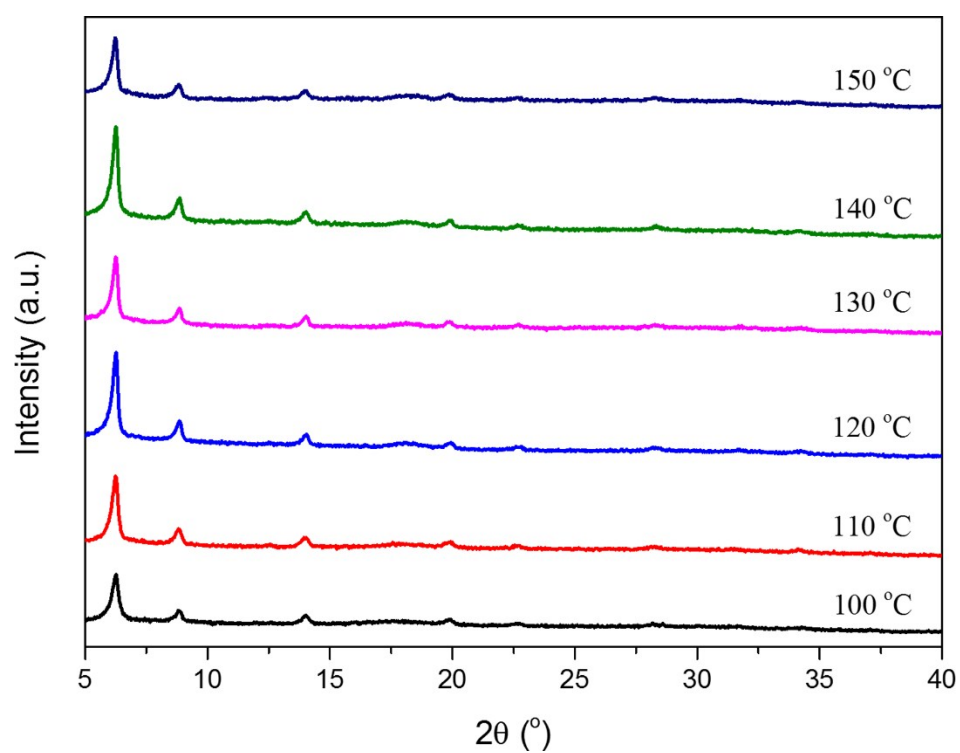


**Fig. S11** XRD patterns of Zr-Fc MOF nanosheets synthesized under different reaction temperature (Run 1-5, 9 at Table S4).

**Table S5** Experimental parameters for the synthesis of Zr-Fc MOF nanosheets under different reaction time (60-150 min).

Runs	ZrCl <sub>4</sub>		Fc(COOH) <sub>2</sub>		CH <sub>3</sub> COOH		DMF	T	t
	mg	mmol	mg	mmol	mL	mmol	mL	°C	min
1	117.9	0.5	138.2	0.5	1.43	25	15	120	<b>60</b>
2	117.0	0.5	137.8	0.5	1.43	25	15	120	<b>70</b>
3	116.7	0.5	137.5	0.5	1.43	25	15	120	<b>80</b>
4	116.9	0.5	136.9	0.5	1.43	25	15	120	<b>90</b>
5	116.8	0.5	137.7	0.5	1.43	25	15	120	<b>100</b>
6	118.0	0.5	137.3	0.5	1.43	25	15	120	<b>110</b>
7	116.2	0.5	137.5	0.5	1.43	25	15	120	<b>120</b>
8	118.6	0.5	137.0	0.5	1.43	25	15	120	<b>150</b>

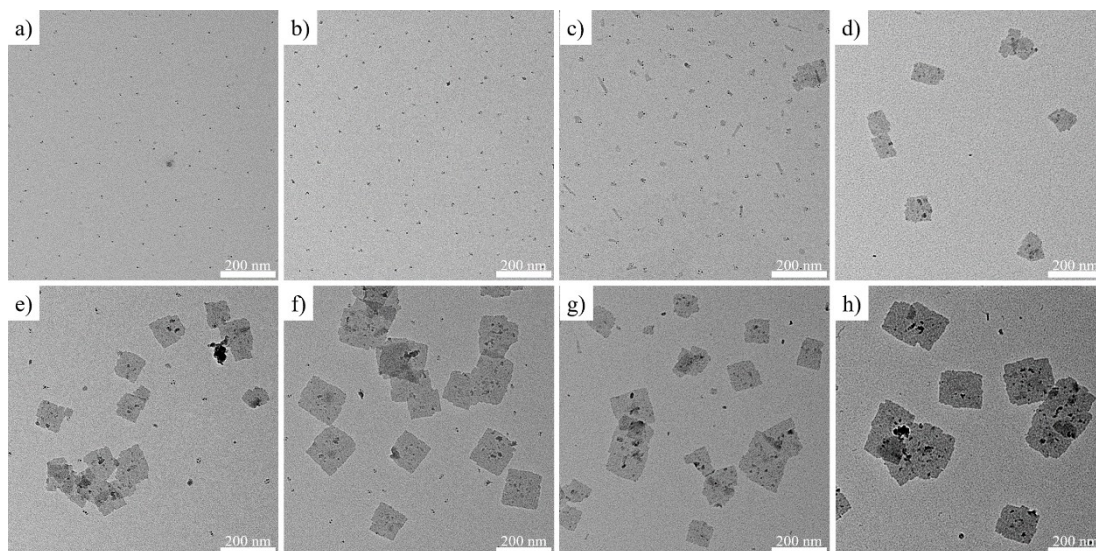


**Fig. S12** TEM images of Zr-Fc MOF synthesized at different reaction time. a) 60 min, b) 70 min, c) 80 min, d) 90 min, e) 100 min, f) 110 min, g) 120 min and h) 150 min (Run 1-8 at Table S5).



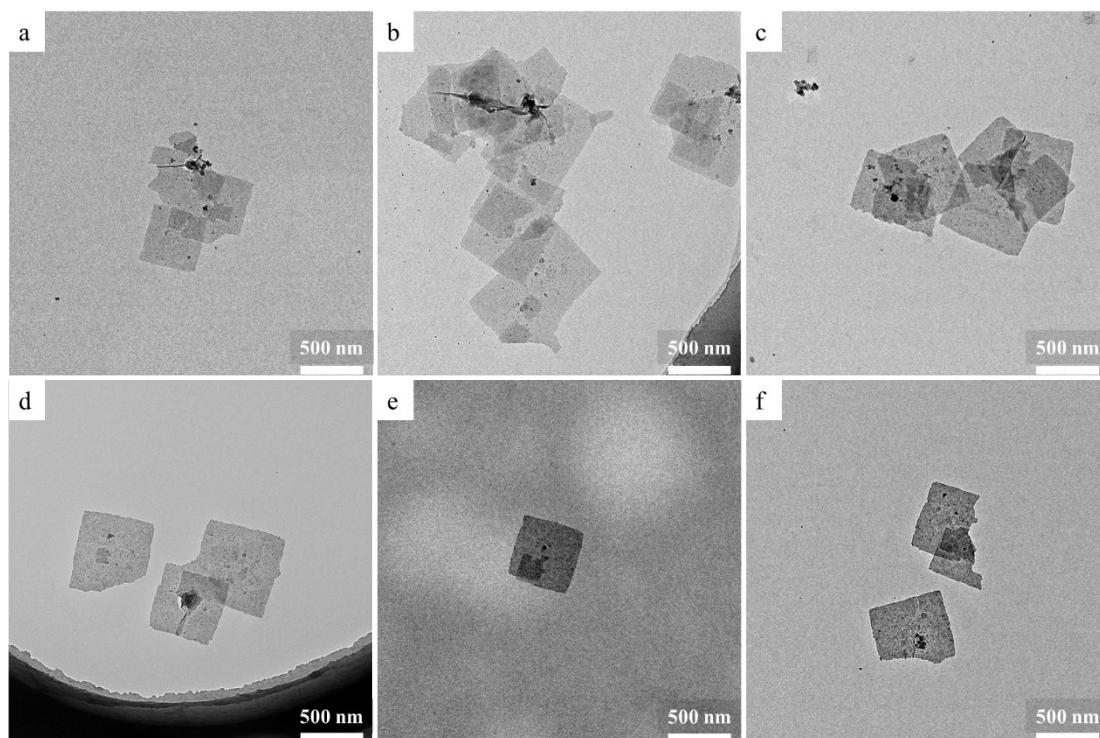


**Fig. S13** TEM images of Zr-Fc MOF nanosheets synthesized under different reaction time. a) 2h, b) 3h, c) 6h, d) 12h, e) 24h and f) 48h (Run 6-11 at Table S4).

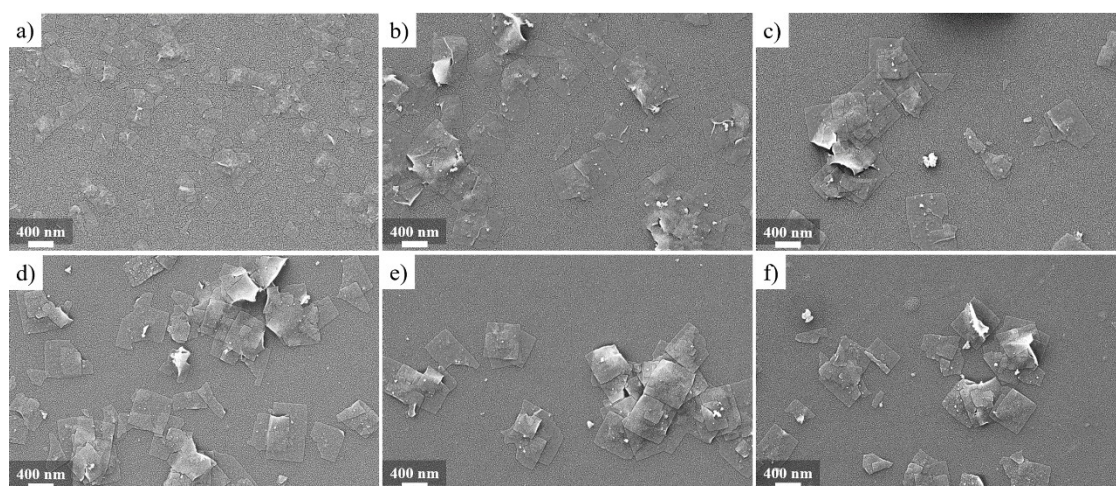


**Fig. S14** SEM images of Zr-Fc MOF nanosheets synthesized under different reaction time. a) 2h, b) 3h, c) 6h, d) 12h, e) 24h and f) 48h (Run 6-11 at Table S4).

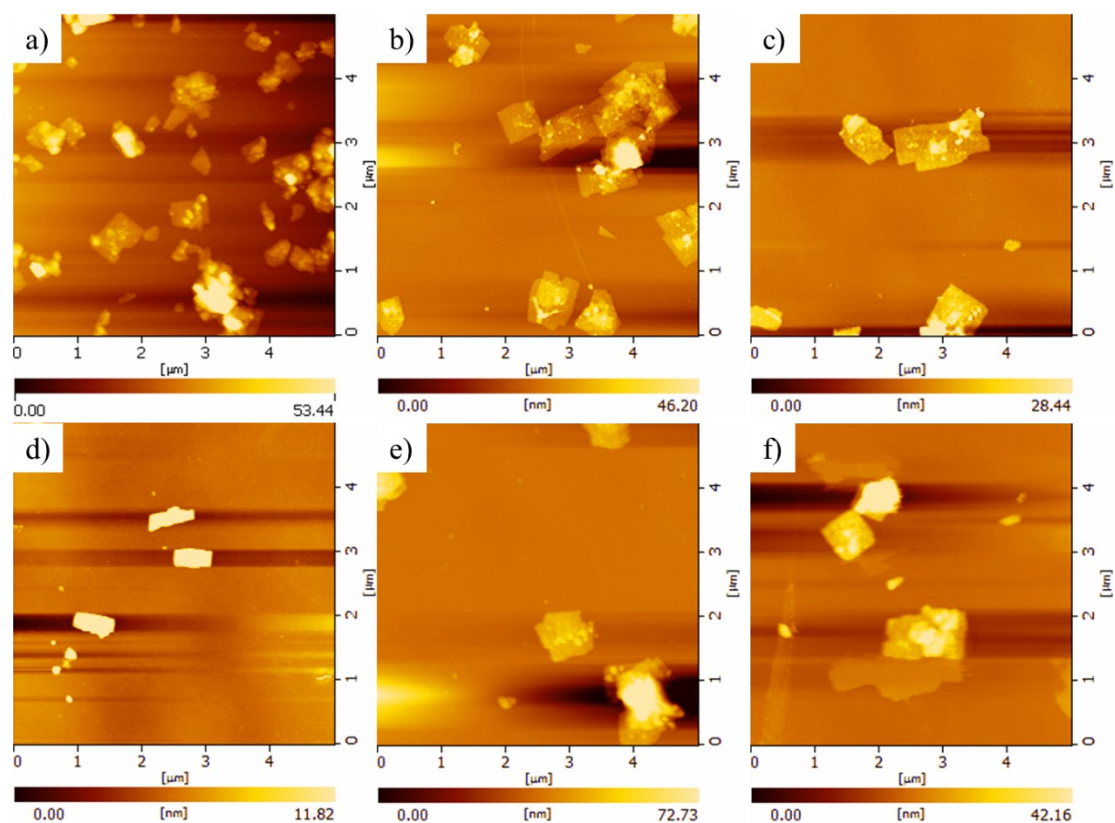


**Fig. S15** AFM height images of Zr-Fc MOF nanosheets synthesized under different reaction time.

a) 2h, b) 3h, c) 6h, d) 12h, e) 24h and f) 48h (Run 6-11 at Table S4).

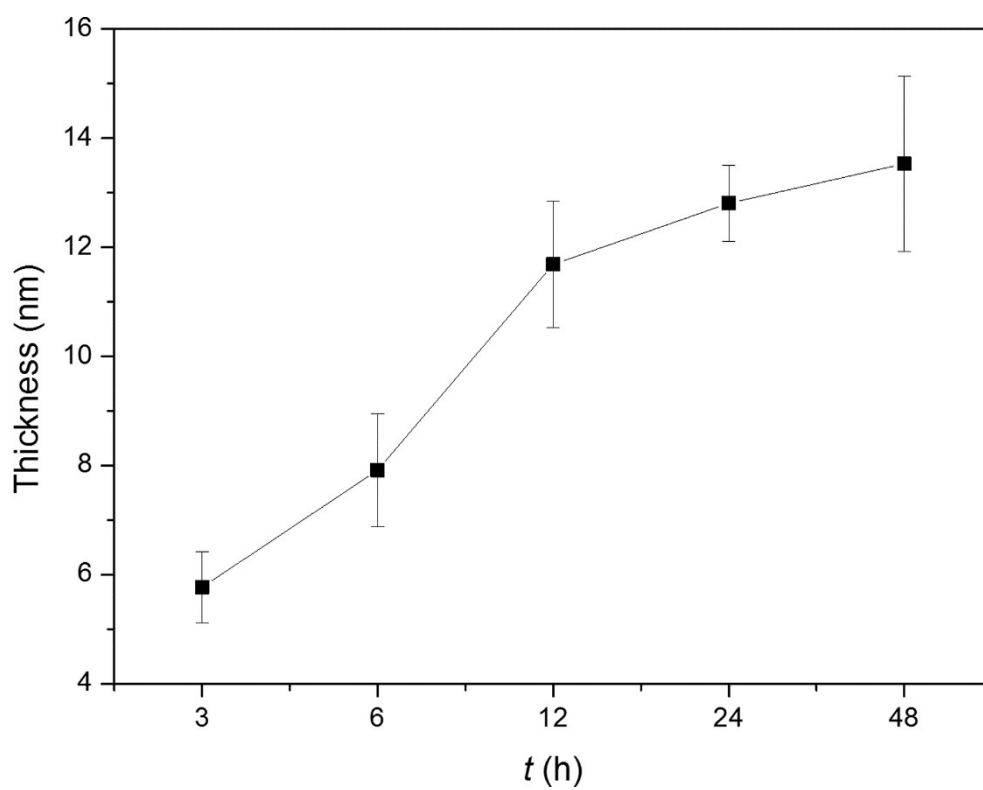


**Fig. S16** Thickness of Zr-Fc MOF nanosheets synthesized under different reaction time.



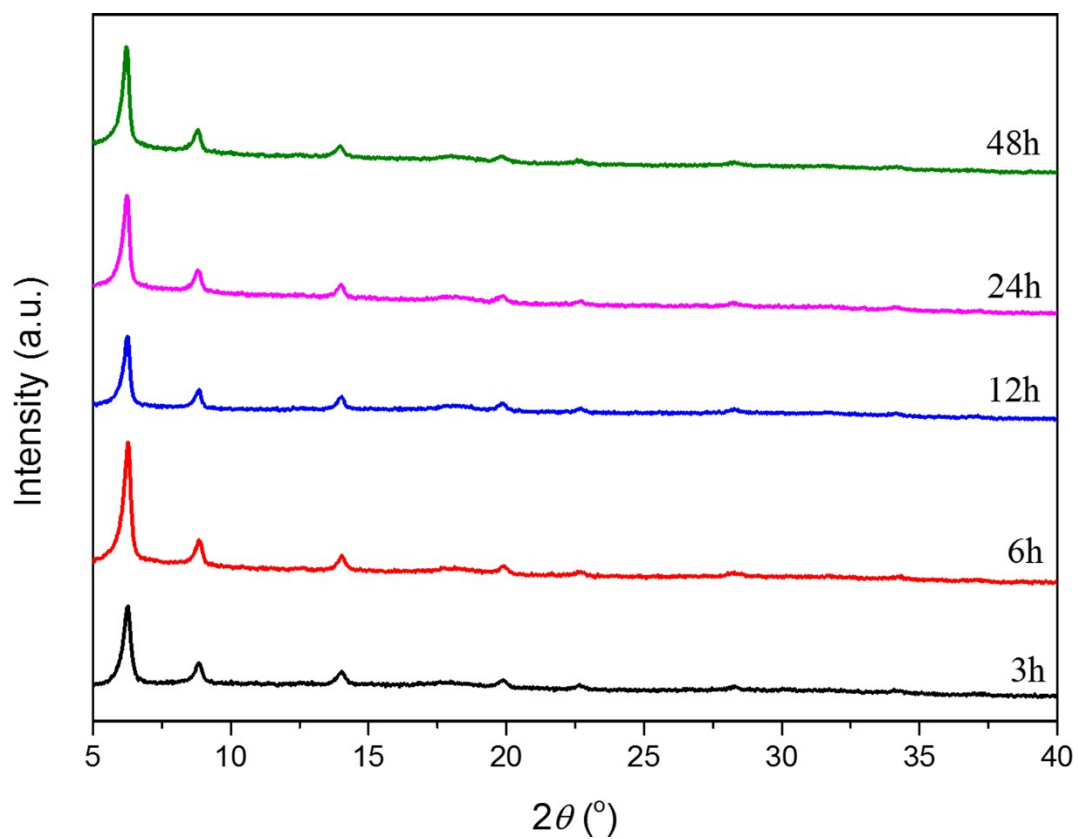


**Fig. S17** XRD patterns of Zr-Fc MOF nanosheets synthesized under different reaction time (Run 7-11 at Table S4).

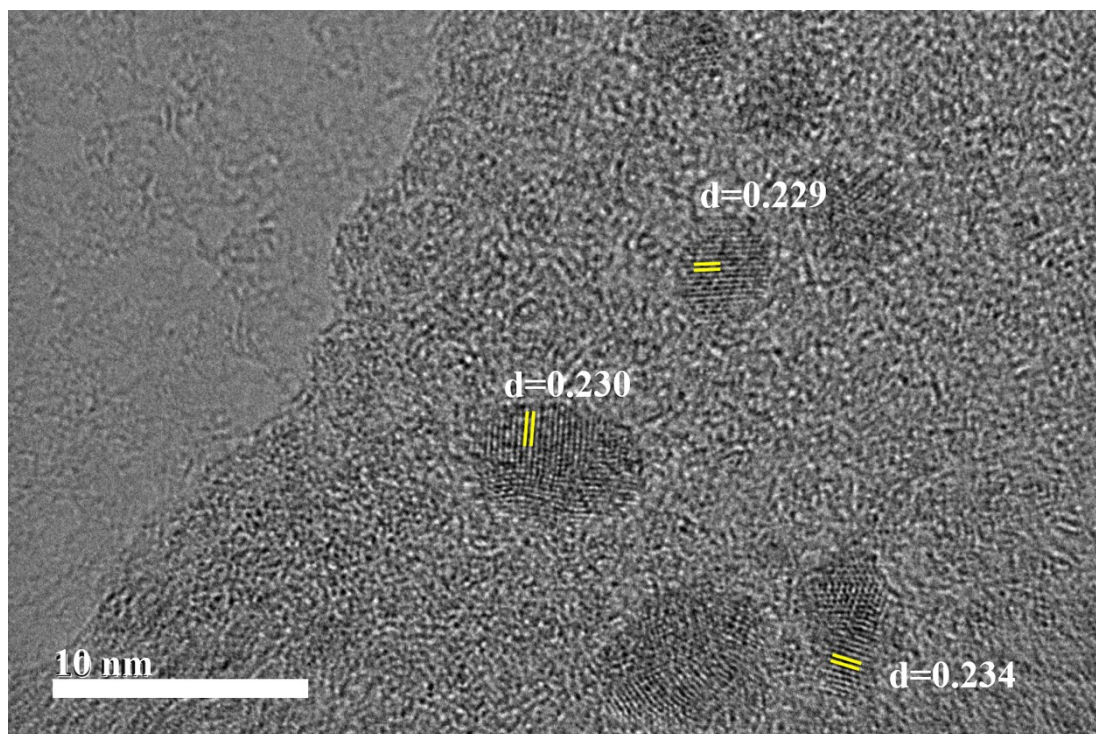


**Fig. S18** HR-TEM image of Pd/Zr-Fc MOF.

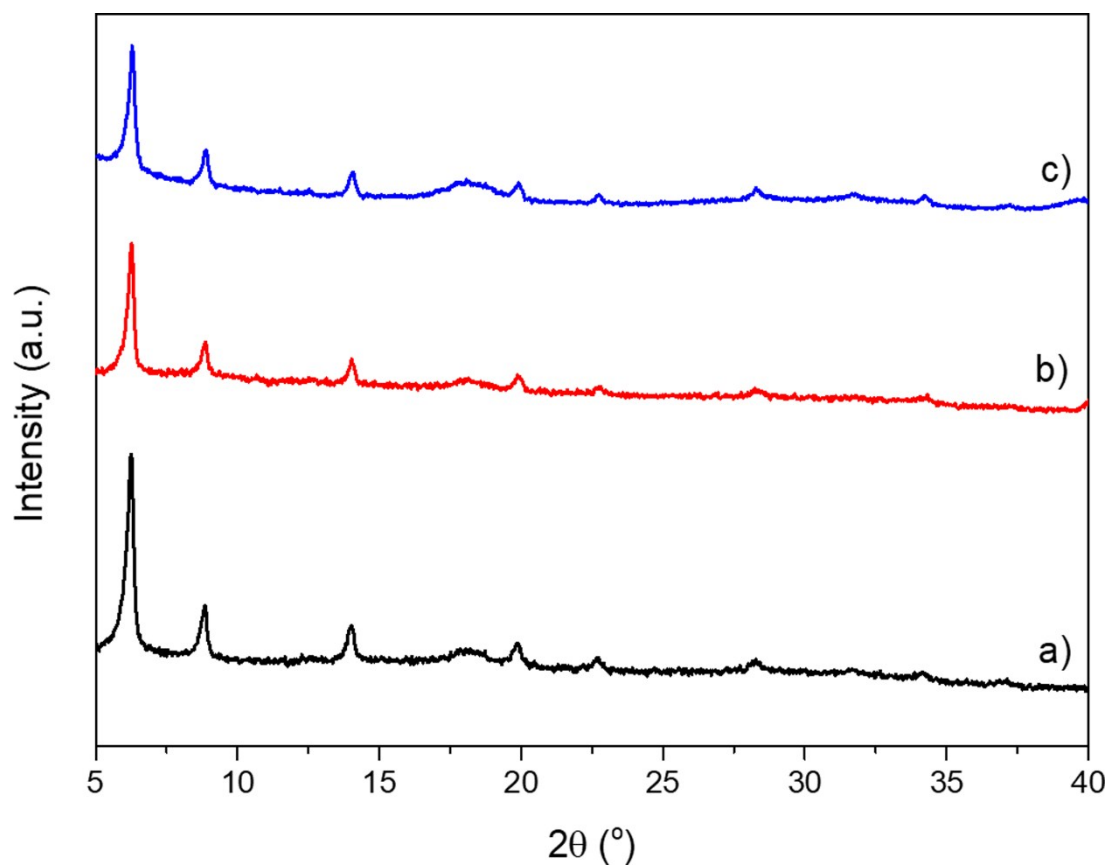


**Fig. S19** XRD patterns of Zr-Fc MOF (a), Pd/Zr-Fc MOF before (b) and after (c) hydrogenation reaction.

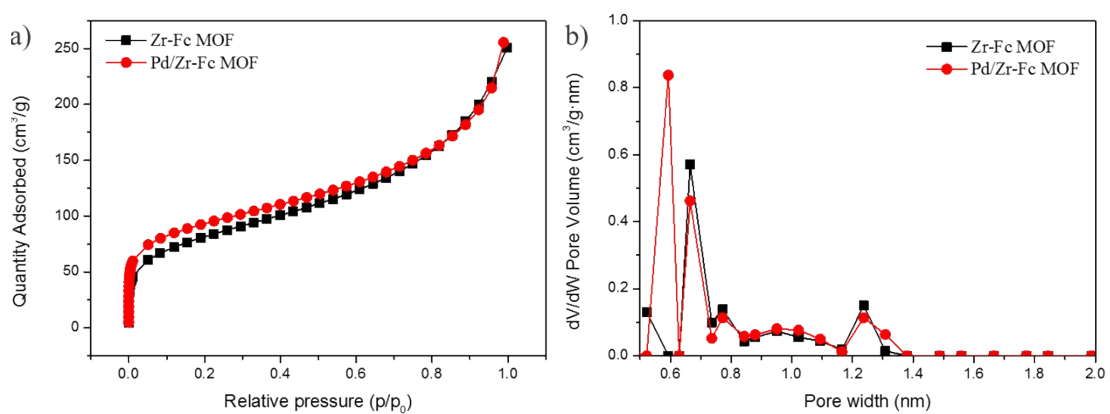


**Fig. S20**  $N_2$  isotherms of Zr-Fc MOF and Pd/Zr-Fc MOF at 77 K. b) Pore-size distributions of Zr-Fc MOF and Pd/Zr-Fc MOF.

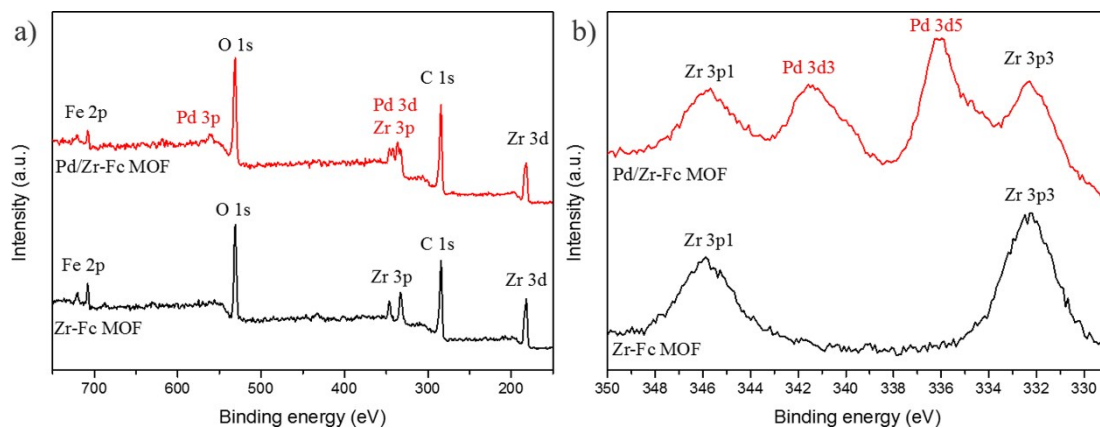


**Fig. S21** a) XPS spectra of Zr-Fc MOF and Pd/Zr-Fc MOF. b) High-resolution XPS Pd 3d and Zr 3p spectra of Zr-Fc MOF and Pd/Zr-Fc MOF.

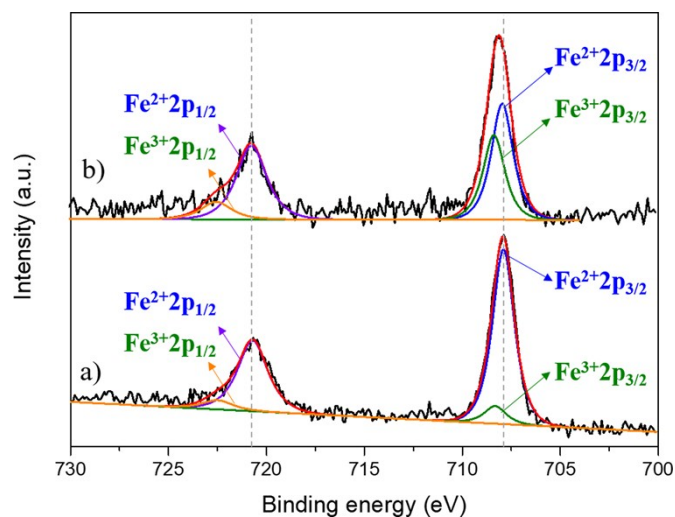


**Fig. S22** High-resolution Fe 2p spectra of Zr-Fc MOF (a) and Pd/Zr-Fc MOF (b).

**Table S6** Quantitative analyses of the XPS survey scans.

Samples	O 1s	C 1s	Pd 3d5	Zr 3d	Fe 2p
Zr-Fc MOF/atom%	31.07	61.62	0	4.56	2.75
Pd/Zr-Fc MOF/atom%	32.02	61.08	0.66	3.66	2.58

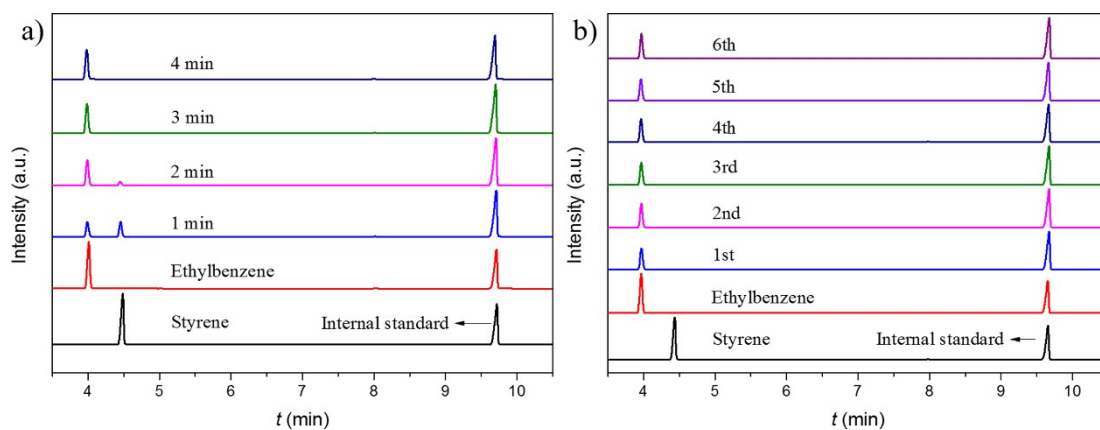


**Fig. S23** GC curves of styrene, ethylbenzene and the solution taken a) after different reaction time b) after 4 min for different reaction cycles. The hydrogenation reaction was catalyzed by Pd/Zr-Fc.

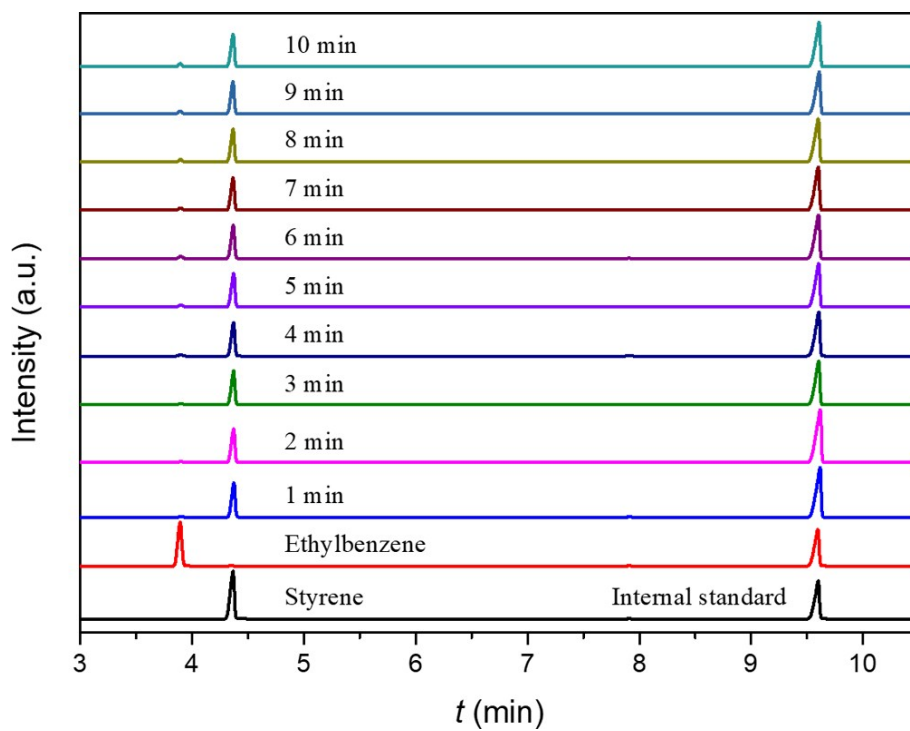


**Fig. S24** GC curves of styrene, ethylbenzene and the solution taken after different reaction time. The hydrogenation reaction was catalyzed by Pd/UiO-66.

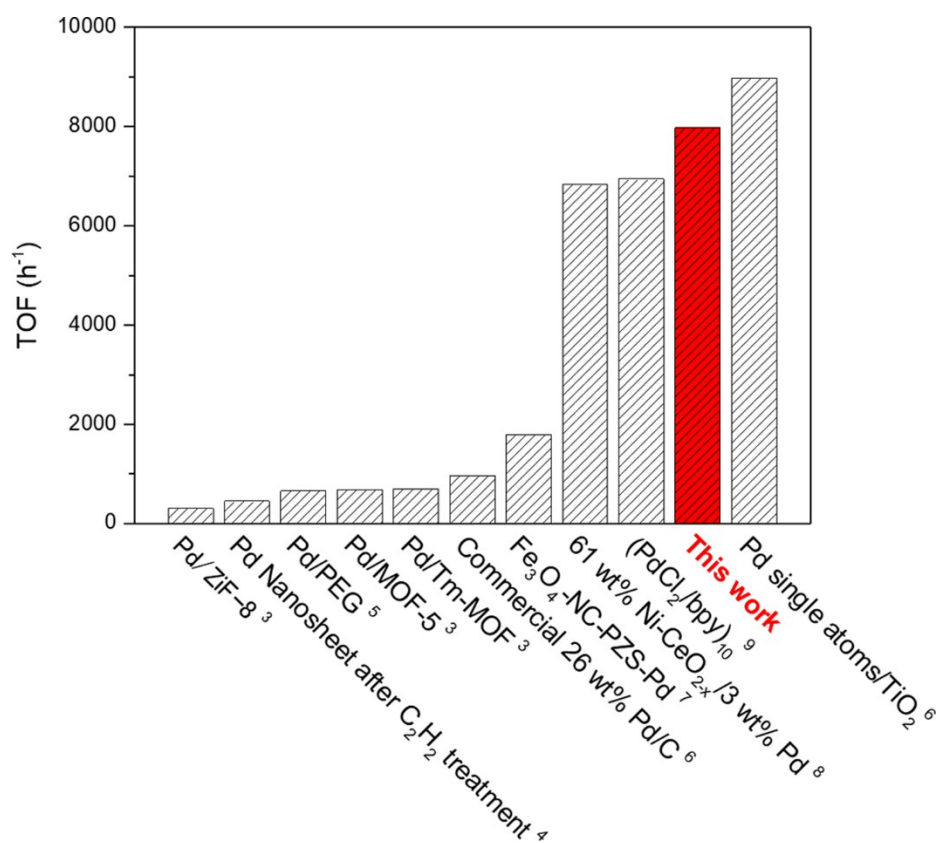


**Fig. S25** Summary of TOF values in the hydrogenation of styrene reaction catalyzed by different Pd-based catalysts from references <sup>3-9</sup>.

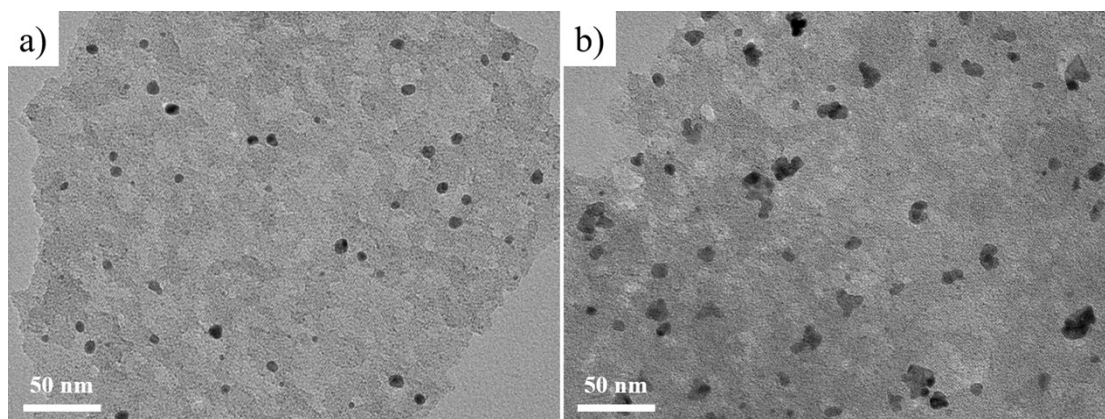


**Fig. S26** TEM images of Pd/Zr-Fc MOF before (a) and after (b) hydrogenation reaction.



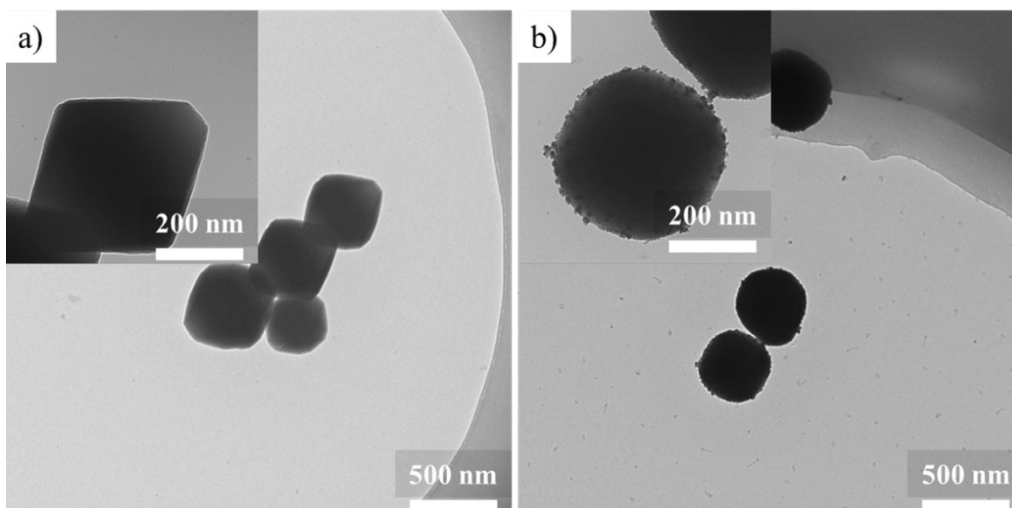


**Fig. S27** TEM images of a) UiO-66 and b) Pd@UiO-66.

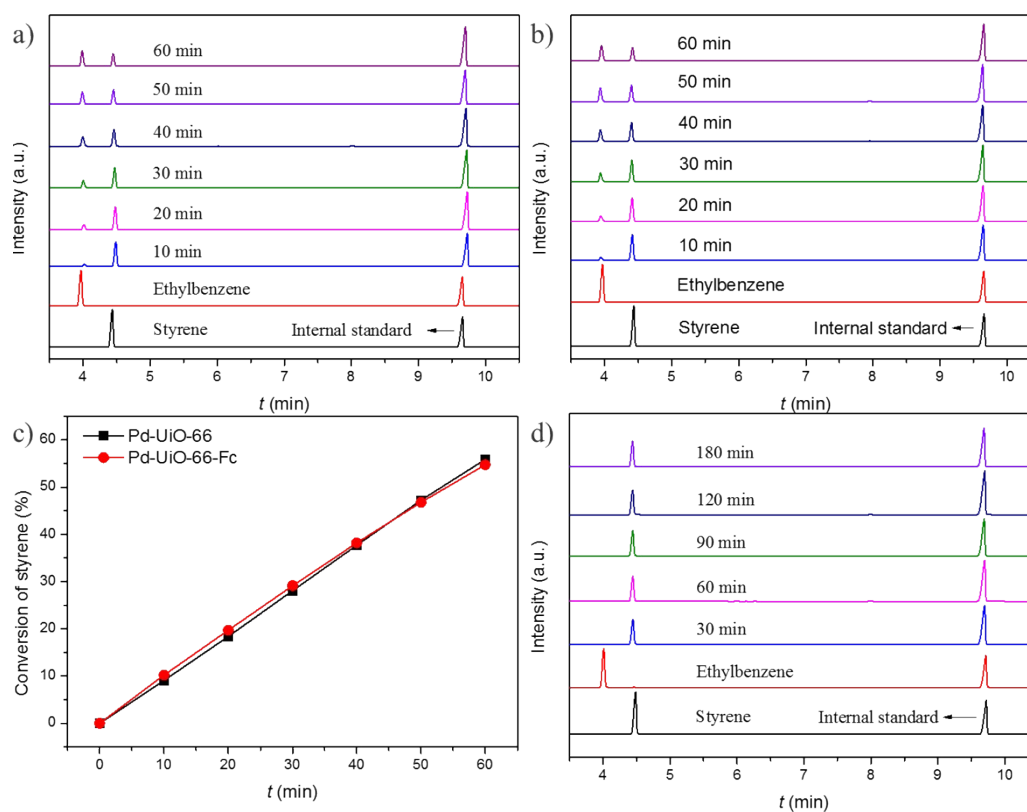


**Fig. S28** GC curves of styrene, ethylbenzene and the solution taken after different times of reaction.

The hydrogenation reaction was catalyzed by Pd/UiO-66 without (a) and with addition of ferrocene (b). c) Conversion of styrene at different reaction time catalyzed by Pd/UiO-66 without (rectangle) and with addition of ferrocene (circle). d) GC curves of styrene, ethylbenzene and the solution taken after different times of reaction catalyzed by Zr-Fc MOF.



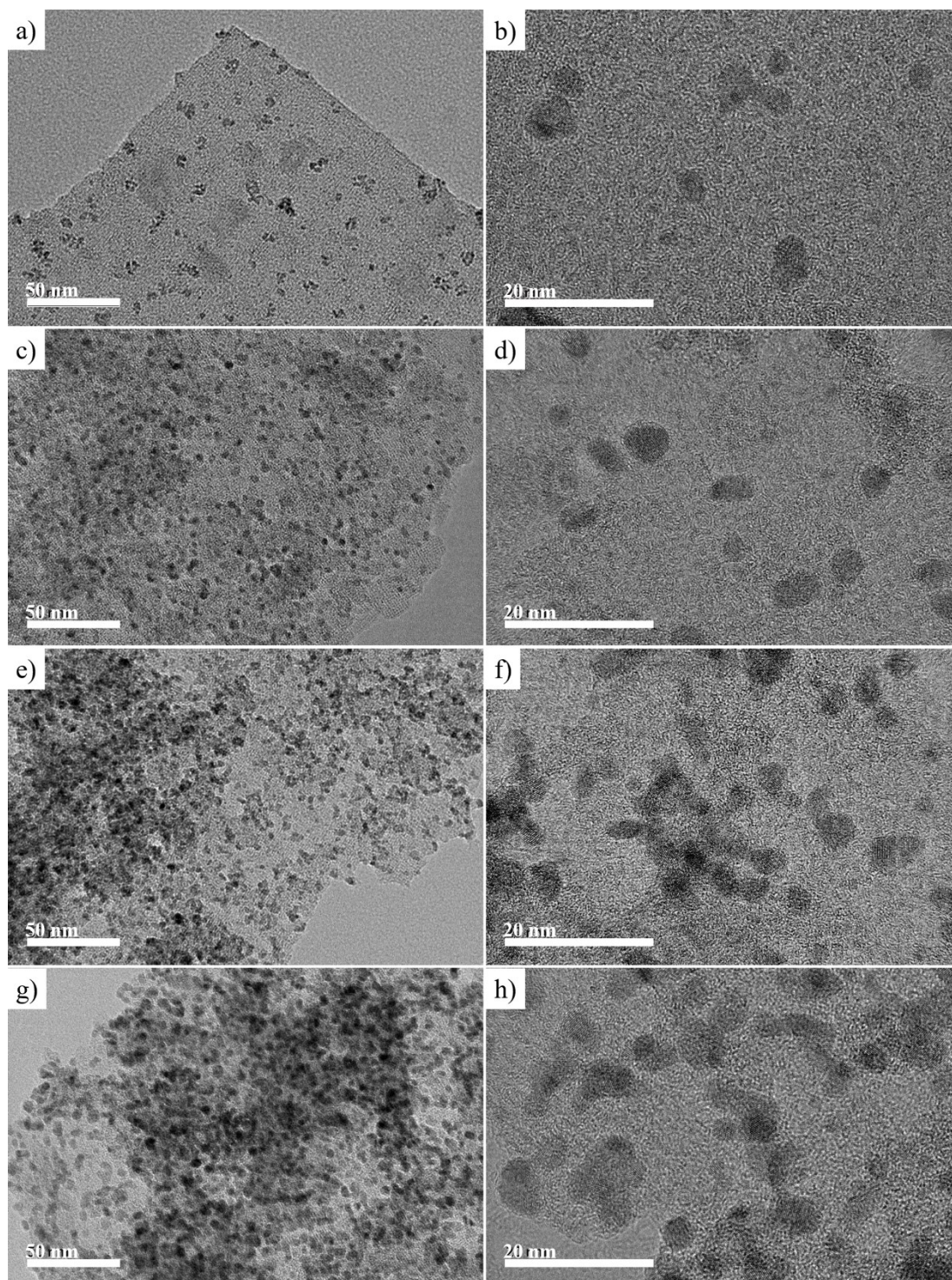


**Fig. S29** TEM images of Pd/Zr-Fc with different Pd content. a) and b) 3.44 wt. %, c) and d) 9.73 wt. %, e) and f) 25.62 wt. %, g) and h) 35.29 wt. %. (Zr-Fc MOFs were synthesized at 120 °C).

**Table S7** Summary of TOF of values in the hydrogenation of styrene reaction catalyzed by Pd/Zr-Fc with different thickness and Pd content.

T <sup>a</sup>	Thickness	Pd content <sup>b</sup>	TOF
°C	nm	wt. %	h <sup>-1</sup>
120	11.6±1.2	3.44	7968
		9.73	7160
		25.62	6703
		35.29	6296
100	4.4±0.8	15.26	7436
150	15.9±1.9	12.58	7117

a: T is the temperature applied during the synthesis of Zr-Fc MOFs to control their thickness.

b: The Pd content of Pd/Zr-Fc MOFs were measured by ICP-AES.

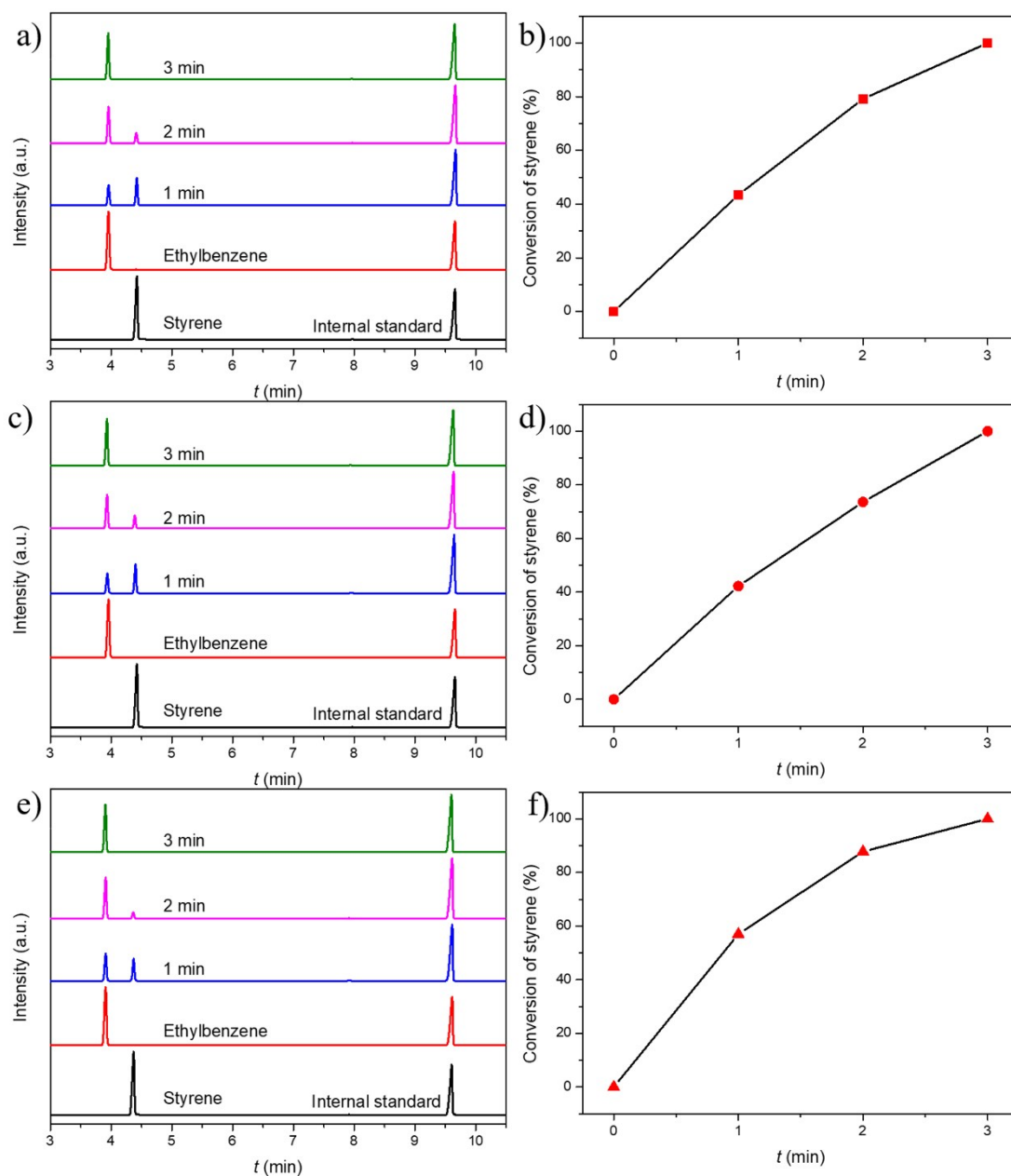


**Fig. S30** GC traces of the hydrogenation of styrene reaction catalyzed by Pd/Zr-Fc MOF with different Pd content. a) 9.73 wt. %, c) 25.62 wt. % and e) 35.29 wt. %. Conversion of styrene at different reaction time catalyzed by Pd/Zr-Fc MOF with different Pd content. b) 9.73 wt. %, d) 25.62 wt. % and g) 35.29 wt. %.



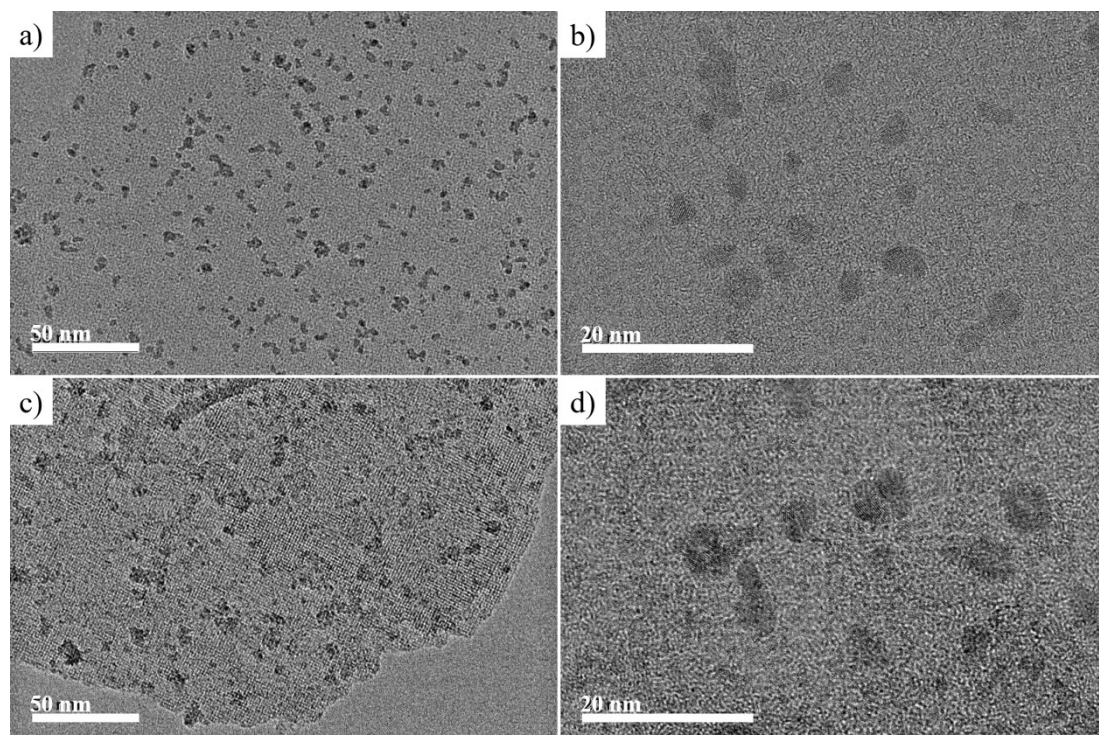


**Fig. S31** TEM images of Pd/Zr-Fc prepared with Zr-Fc MOF synthesized at different temperature.

a) and b) 100 °C, c) and d) 150 °C

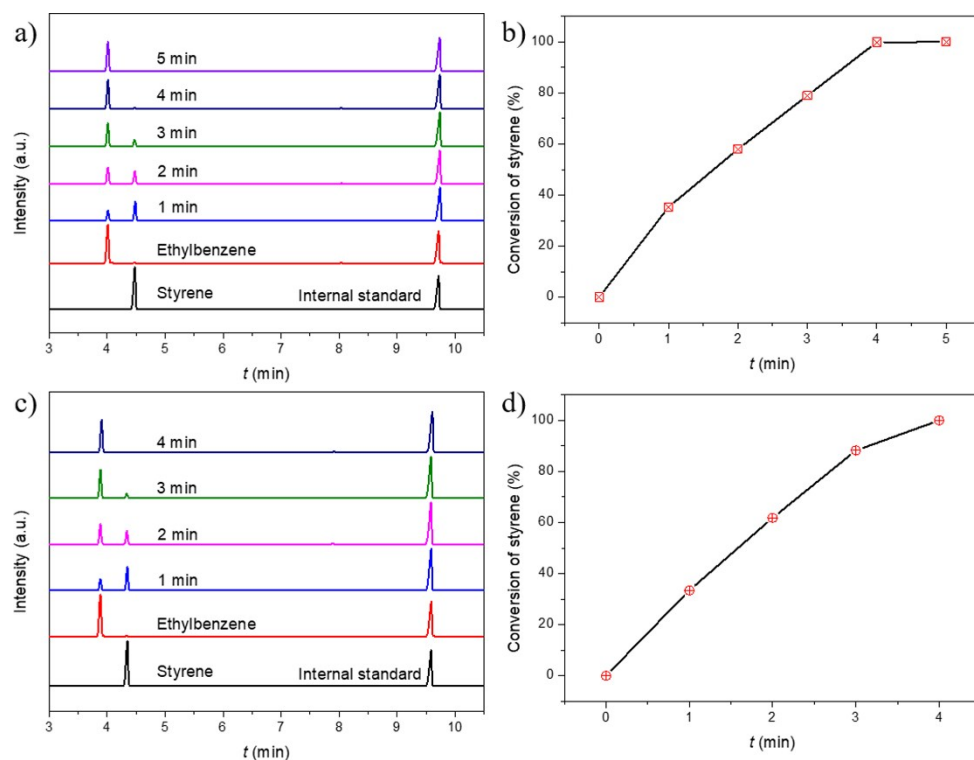


**Fig. S32** GC traces of the hydrogenation of styrene reaction catalyzed by Pd/Zr-Fc MOF with different Zr-Fc MOF thickness. a) 4.4 nm and c) 15.9 nm. Conversion of styrene at different reaction time catalyzed by Pd/Zr-Fc MOF with different Zr-Fc MOF thickness. b) 4.4 nm and d) 15.9 nm.

## Reference

1. G. Huang, Q. Yang, Q. Xu, S.-H. Yu, H.-L. Jiang, *Angew. Chem. Int. Ed.* **2016**, *55*, 7379.
2. J. Ma, A. G. Wong-Foy, A. J. Matzger, *Inorg. Chem.* **2015**, *54*, 4591.
3. Y. Pan, D. Ma, H. Liu, H. Wu, D. He, Y. Li, *J. Mater. Chem. A* **2012**, *22*, 10834.
4. Y. Dai, S. Liu, N. Zheng, *J. Am. Chem. Soc.* **2014**, *136*, 5583.
5. F. A. Harraz, S. E. El-Hout, H. M. Killa, I. A. Ibrahim, *J. Cat.* **2012**, *286*, 184.
6. P. Liu, Y. Zhao, R. Qin, S. Mo, G. Chen, L. Gu, D. M. Chevrier, P. Zhang, Q. Guo, D. Zang, B. Wu, G. Fu, N. Zheng, *Science* **2016**, *352*, 797.
7. S. Yang, C. Cao, Y. Sun, P. Huang, F. Wei, W. Song, *Angew. Chem. Int. Ed.* **2015**, *54*, 2661.
8. Y.-F. Jiang, C.-Z. Yuan, X. Xie, X. Zhou, N. Jiang, X. Wang, M. Imran, A.-W. Xu, *ACS Appl. Mater. Interf.* **2017**, *9*, 9756.
9. S. Gao, W. Li, R. Cao, *J. Colloid Interf. Sci.* **2015**, *441*, 85.